

## Photo-neutron emission mechanism at low-energy photon interaction

Mahdi Bakhtiari<sup>a</sup>, Nam-Suk Jung<sup>b</sup>, Hee-Seock Lee<sup>a,b\*</sup>

<sup>a</sup>Division of Advanced Nuclear Engineering, POSTECH, Pohang 37673, Republic of Korea

<sup>b</sup>Pohang Accelerator Laboratory, POSTECH, Pohang 37673, Republic of Korea

\*Corresponding author: [lee@postech.ac.kr](mailto:lee@postech.ac.kr)

### 1. Introduction

Photoneutrons are of importance as they can result in radiological concerns in radiation protection. Photonuclear reactions are used as neutron sources for neutron imaging techniques such as Bragg edge imaging. A photonuclear reaction consists of the photoabsorption process and particle emission [1]. Photon is absorbed by the target via giant-dipole resonance (GDR) and quasi-deuteron (QD). For photon energies lower than 30 MeV, the photoabsorption is determined by GDR and up to around 150 MeV, it is described by QD [2]. When the photon is absorbed, the target nucleus is excited and decays via direct, preequilibrium and compound mechanisms. In direct reactions, the residual nucleus is left in the ground or first excited states so that the emitted neutrons form the high energy part of the spectrum. Preequilibrium mechanism becomes important at photon incident energies above 10 MeV. The emitted particle resulted from the preequilibrium mechanism forms the emission spectra between compound and direct mechanisms.

Here the contribution of each reaction mechanism is shown. The neutron production yields from  $^{197}\text{Au}(\gamma, xn)$  reaction were also calculated using Monte Carlo and are compared with the experimental data by Tuyet et al. [3].

### 2. Methods and Results

TALYS-1.95 [4] was used to calculate the double differential cross sections (DDX) of  $^{197}\text{Au}(\gamma, xn)$  reaction to illustrate the contributions of abovementioned mechanisms and the results are shown in Fig. 1. These results illustrate that the compound mechanism is dominant up to 4 MeV for this reaction. After that the preequilibrium becomes important in the neutron emission process. The direct contribution is very small. The Monte Carlo codes PHITS-3.1 [5], FLUKA 4-2.1 [6] and MCNP6.1 [7] were used to calculate the neutron production yields. Two photonuclear cross section libraries, ENDF/B-VII.0 [8] and IAEA/PD-2019 [9] as well as physics models were used in MCNP6.1. By using the physics model in MCNP, the Lorentzian function is used at the giant dipole region (GDR) for calculating the photonuclear cross sections. The total photonuclear cross sections are evaluated in JENDL/PD-2004 [10] library and are used in the PHITS code. The neutron production from excited nucleus is estimated by Generalized Evaporation Model (GEM) [11]. FLUKA uses the IAEA

photonuclear cross section library as well as other experimental data [12] and cannot be manipulated by the user. In a case that the library does not have the photonuclear cross sections, they are calculated based on the Lorentzian function at the GDR. After the photon is absorbed by the nucleus, nuclear effects on the initial and final state such as reinteraction or emission of reaction products are considered in FLUKA hadronic interaction model PreEquilibrium Approach to Nuclear Thermalization (PEANUT) [6]. In the simulations, a cylindrical target with thickness and diameter of 1 cm was irradiated with 16.6-MeV monoenergy photons. The results were calculated at 30°, 60°, 90°, 120° and 150°, which are the angles between detectors and photon beam. In the simulations, the polarized photons cannot be defined so as the photon beam is unpolarized. The calculated results were compared with the experimental data [3] and the results of 30° are only shown in Fig. 2.

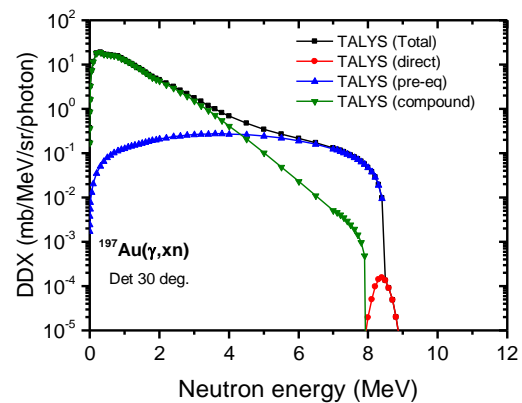


Fig. 1. Contribution of compound, preequilibrium and direct mechanisms to the DDX calculated by TALYS.

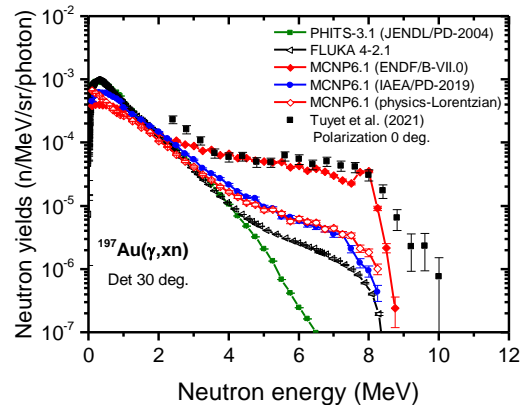


Fig. 2. Experimental and calculated photoneutron production yields at 30° from  $^{197}\text{Au}$  target induced by 16.6-MeV photons.

The comparison of the calculated neutron yields at different angles and for other materials are discussed and compared with the measured data [3,13] and can be found in our previous work [14].

The data by Tuyet et al. were measured using polarized photons with the polarization angle of  $0^\circ$  as indicated in Fig 2. It is seen that all codes show the compound (evaporation) part of the spectrum. Generally, MCNP6.1(ENDF/B-VII.0) is more consistent with the experimental data up to 8 MeV. PHITS data drop at 4 MeV because it does not consider the preequilibrium mechanism at this incident photon energy. FLUKA, MCNP6.1(IAEA/PD-2019) and MCNP6.1(physics-Lorentzian) are higher than PHITS data as they consider preequilibrium into account. However, they are still lower than the experimental data. All codes failed to reproduce the experimental data above 8 MeV which are related to the direct mechanism.

### 3. Conclusions

Contributions of compound, preequilibrium and direct mechanisms to the photoneutron emission were investigated. The preequilibrium mechanism becomes important above neutron emission energy of 4 MeV for  $^{197}\text{Au}(\gamma, xn)$  reaction. MCNP6.1(ENDF/B-VII.0) could reproduce experimental data well up to 8 MeV. All codes could not reproduce the high energy emitted neutrons. It is concluded that the nuclear data libraries and nuclear models describing photonuclear reactions need to be improved especially above the evaporation part.

### REFERENCES

- [1] H. Sato, T. Sasaki, T. Moriya, et al., Phys. B Condens. Matter 551 (2018).
- [2] M. B. Chadwick, P. G. Young, R. E. MacFarlane, et al., Nucl. Sci. Eng. 144 (2003).
- [3] T. Kim Tuyet, T. Sanami, H. Yamazaki, et al., Nucl. Instruments Methods Phys. Res. Sect. A 989 (2021).
- [4] A. Koning, S. Hilaire, S. Goriely, User Manual of TALYS-1.95(2019).  
<http://www.talys.eu/download-talys>.
- [5] T. Sato, Y. Iwamoto, S. Hashimoto, et al., J. Nucl. Sci. Technol. 55 (2018).
- [6] G. Battistoni, T. Boehlen, F. Cerutti, et al., Ann. Nucl. Energy. 82 (2015).
- [7] J. T. Goorley, M. R. James, T. E. Booth, et al., Initial MCNP6 Release Overview-MCNP6 Version 1.0 (2013).
- [8] D. A. Brown, M. B. Chadwick, R. Capote, et al. Nucl. Data Sheets. 148 (2018).
- [9] T. Kawano, Y. S. Cho, et al., Nucl. Data Sheets. 163 (2020).
- [10] N. Kishida, T. Murata, T. Asami, et al., JENDL Photonuclear Data File, AIP Conf. Proc. 769, 199 (2005).
- [11] S. Furihata, Statistical Analysis of Light Fragment Production from Medium Energy Proton-Induced Reactions, Nucl. Instruments Methods Phys. Res. Sect. B 171, 251 (2000).
- [12] A. Fassò, A. Ferrari, and P. R. Sala, Photonuclear Reactions in FLUKA: Cross Sections and Interaction Models, AIP Conf. Proc. 769, 1303 (2005).
- [13] Y. Kirihara, H. Nakashima, T. Sanami, et al., J. Nucl. Sci. Technol. 57 (2019).
- [14] M. Bakhtiari, N. S. Jung, and H. S. Lee, Nucl. Instruments Methods Phys. Res. Sect. B (2022). In publication.